Experimental Evaluation of MIMO Channel Capacity for Wireless Communication Channels

Shailesh, Vanshika Bhateja, Puneet Sehgal, Vipul Kaushal, and Kamlesh Patel*

Department of Electronic Science, University of Delhi South Campus, New Delhi, 110021, India

Volume 1, Issue 6, December 2024
Received:21 September, 2024; Accepted: 16 November, 2024
DOI: https://doi.org/10.63015/10se-2443.1.6

**Correspondence Author Email: kpatel@south.du.ac.in*

Abstract: This research evaluates the channel capacity (CC) of 5th Generation Multiple Input Multiple Output (MIMO) antennas for propagation channels used in wireless communication. In the presence of several frequency sources for the information and communication channels, the effect on the CC of one-port and multi-port antennas is observed using the Path Loss Model (PLM), which is significantly impacted due to the number of antennas used and their characteristics. The CC is also estimated using a different approach, Kronecker's Model (KM). The channel matrix using both models is estimated by maintaining 5 cm and 25 cm spacing between the transmitting and receiving antennas. At 2.4 GHz for a 1-port antenna-based channel, the CC calculated using PLM is 5.5 bps/Hz for both spacing, whereas the CC calculated using KM is 3.65 bps/Hz and 3.12 bps/Hz for 5 cm and 25 cm spacing, respectively. The CC in the PLM is found between 35 to 140 bps/Hz at a frequency of 3.5 GHz, whereas it is reported between 12 to 38 bps/Hz using the KM at the same frequency, irrespective of distances. The maximum CC calculated using PLM is 5 bps/Hz for a 1-port antenna-based channel, 34 bps/Hz for 2-port MIMO antenna-based channels, 80 bps/Hz for 4-port MIMO antenna-based channels, and 157 bps/Hz for 8-port MIMO antenna based channels in the frequency band from 3.45 GHz to 3.7 GHz. Thus, it is experimentally confirmed that the capacity enriched by approximately 4 times on increasing the number of antenna ports from 2 to 8 and operating frequency.

Keywords: Channel capacity, WLAN, 5G, MIMO, SISO, Signal to Noise Ratio (SNR).

1

1. Introduction: The rise of wireless personal communication systems (PCS) can be ascribed to the increasing demand for technological breakthroughs that more closely correspond with the swiftly evolving demands of our surroundings [1]. The idea of information and communication propagation channels, which have a wide range of applications in security, entertainment, healthcare, and communication, was conceived by one of the numerous inventive PCSs. Wireless communication networks such as Wireless Local Area Networks (WLAN), Worldwide Interoperability for Microwave Access (WiMAX), and 5G have been widely utilised by portable wireless communication devices. These are the most well-documented wireless bands used with MIMO antenna systems for large throughput [2]. Several MIMO antenna approaches have been developed recently to meet the requirements of the wireless communication system's channel capacity (CC) and data transmission rate [3]. Benefits of MIMO in WLAN and 5G technologies include faster data rates, a single connection, lower latency, and more connected nodes. The increasing demand for higher data rates has prompted the development of new techniques aimed at achieving these speeds. Unlike typical wireless propagation channels, the estimation of its characteristics in information and communication is influenced by the kind, orientation, propagation environment, and number of antenna elements [1].

Recently, a dielectric medium-equipped four-port integrated MIMO antenna construction

operating at 2.4 GHz was presented in [4]. By raising the pattern gain, the achievable CC (21 bps/Hz) was greater than the optimum CC. A dual-band 4-port MIMO antenna operating at 28 GHz and 41.69 GHz was proposed [5]. After evaluation, the CC was found to be nearly equal to 21 bps/Hz. A quad-port MIMO antenna with a 2.42–7.45 GHz bandwidth was suggested [6]. Considering that the four elements had different numbers of transmitting and receiving antennas, their maximum CC was 21.34 bps/Hz. A quad-element MIMO antenna for the 433 MHz industrial, scientific, and medical (ISM) bands was designed [7]. Moreover, this antenna offered 19.9 bps/Hz of CC. A range of the computed CC was reported 57.98 to 59.87 bps/Hz in a 12× 12 MIMO antenna system made using four tri-port antennas [8]. A weighted polarisation MIMO antenna was used for 2.45 GHz wireless body area networks [9]. The average CC that was computed was 16 bps/Hz. In all the above-reported studies, CC is plotted by adjusting signal-to-noise ratio (SNR) values from 1 dB to 20 dB or taking any constant SNR value. So, there is very little information about the measurement of SNR, as well as the measurement of path loss and channel matrix [6].

This research uses a Spectrum Analyzer to obtain the received power and SNR which are used to evaluate the CC of WLAN/5G MIMO antennas under two different models: the Path Loss Model (PLM) and the Kronecker Model (KM). Additionally, by putting 1-port, 2-port, 4-port, and 8-port antennas at both the transmitting (T_x) and receiving (R_x) sides, the CC has been assessed. To the best of the authors' information, no thorough investigation has been done on the SNR and CC measurement for WLAN/5G MIMO. The rest of the research paper is structured as follows. The specifications of the measurement setup are highlighted in Section 2. The channel model and capacity estimates are provided in Section 3. In Section 4, the measured data for the SNR and CC are presented. In Section 4, the suggested work is also contrasted with other reported work. The conclusion is provided in Section 5.

2. Measurement Setup: Three antennas, a 1-port circular spilt-ring resonator (SRR) antenna [10] (Ant. 1) for the WLAN band measurements over frequency band 2.29-2.95 GHz, a 2-port dual polarized circular slot microstrip antenna [11] (Ant. 2), and 8-port circular slot microstrip MIMO antenna [12](Ant. 3) for 5G band measurements over the frequency band 3.4-3.7 GHz are selected to form channels. These antennas are shown in Figure 1(a)-(c), respectively. These antennas provide sufficient gain and radiation properties in the entire WLAN (Ant. 1) and 5G band (Ant. 2, and Ant. 3). The ANSYS 3D High-Frequency Simulation Software (HFSS) is used for designing Ant. 1 and CST studio suite is for designing Ant. 2 and Ant. 3. These antennas are made on an FR4 substrate with 4.4 dielectric constant. The FR4 substrate is chosen for the antennas used because it is lightweight, cheap, and easily accessible, and its hardness makes this substrate immune to environmental changes. The main drawback of FR4 is that the copper coating on the FR4 substrate can be chipped off over time. The complete dimensions of the antennas used are shown in Table 1 and their performance parameters are presented in Table 2.

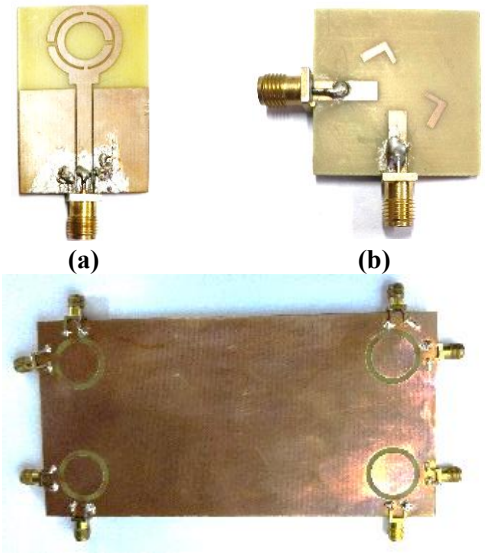

Figure 1: Fabricated picture of the antennas used (a) Ant. 1, (b) Ant. 2, and (c) Ant. 3.

An anechoic chamber was used for all the measurements, which has a size of 5.8m×2.7m×3.05m. This anechoic chamber has a Quiet Zone of size 0.4m×0.4m×0.4m, which provides a reflectivity level from -34.24 dB to -48.51 dB and shielding effectiveness from -86 dB to -90 dB in the frequency range 800 MHz -16 GHz. The standard used for the measurement is a ridge horn antenna. For all the measurements, two arbitrary distances (D) between identical transmitting and receiving antennas are selected as 5 and 25 cm, so the effect of distance over the CC can be observed in near-field and far-field regions.

Table 1: Complete dimensions of the antennas used

Antenna No.	Ant. 1	Ant. 2	Ant. 3
Feed (mm^2)	22×3	11.9×3.5	11.9×3.5
Radius of the circular ring/slot (mm)	7.5 (external ring), 5.5 (internal ring)	8.1 (circular slot)	8.1 (circular slot)
Thickness of the circular ring/slot (mm)	1 (both rings)	1.6 (circular slot)	1.6 (circular slot)
Ground (mm^2)	22×11	3.5×3.5	150×75
L-shaped structure	-	(5.5×1.5)+ (4.5×1)	(5.5×1.5)+ (4.5×1)

Table 2: Performance details of the antennas used

Antenna No.	Ant. 1	Ant. 2	Ant. 3
No. of ports	1	2	4/8
Structure of Antenna	Circular SRR	Circular Slot MIMO	Circular Slot MIMO
Frequency range (GHz)	2.29-2.95	3.4-3.7	3.4-3.8
Isolation (dB)	Not Applicable	-44.53	-12
Gain (dB)	2.1	3.77	5.21
Dimension (mm×mm)	43 ×26	35×35	75×150

For the measurements of signal-to-noise ratio (SNR) at these two distances, a RIGOL signal generator model DSG3060 is used to transmit the signal at the desired bands and an R&S spectrum analyzer model FSL6 is used to measure the SNR. To obtain the path loss values, an R&S handheld vector network analyser (VNA) ZVH8 is used for obtaining measured S-parameters for different sets of Ant. 1, Ant. 2, and Ant. 3 [11].

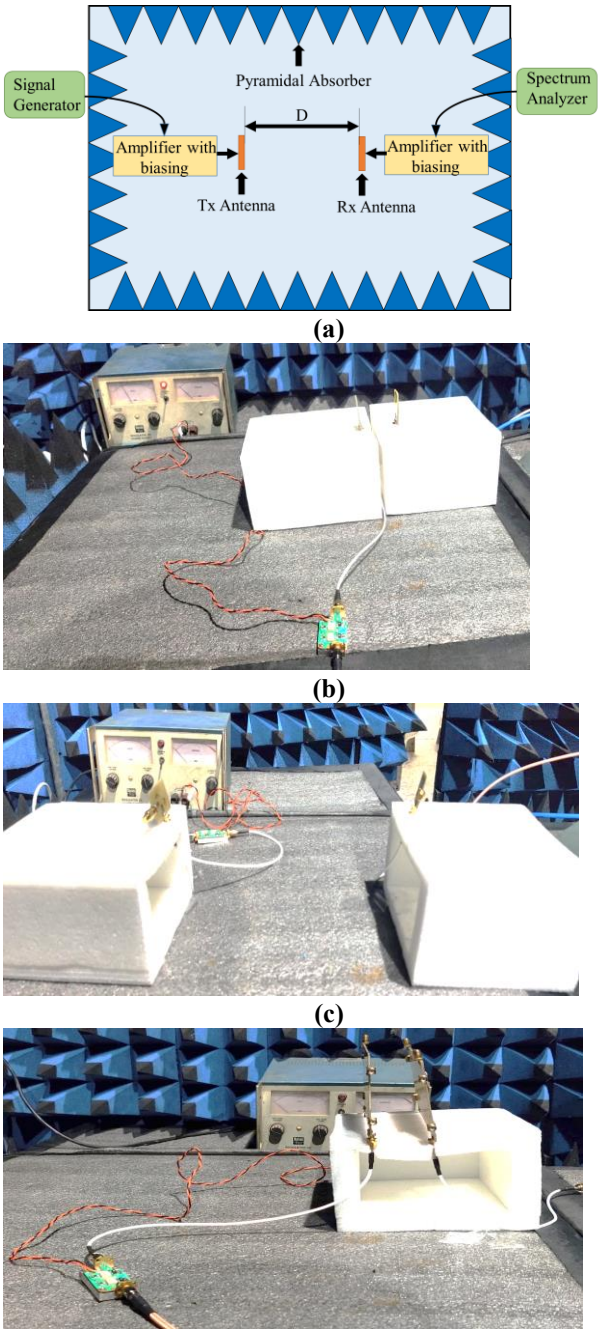

Figure 2: SNR measurement arrangements for (a) Block diagram, (b) Ant. 1 as 1T×1R at 5 cm, (c) Ant. 2 as 2T×2R at 25 cm, and (d) Ant. 3 as 8T×8R at 5 cm.

The channel (H)-matrix for channels made using these antennas is calculated from the respective path loss values using equation (2). Figure 2 illustrates a signal-to-noise ratio (SNR) measurement setup of how the antennas were placed for the wireless communication channels. An amplifier (green-colored circuit) is used to amplify the received signal and then measured on the spectrum analyzer. Since the transmission coefficient is a ratio, the gain of the signal due to this amplifier is nullified as appears equally in the incident and transmitted signals.

3. Characterization of MIMO Channel

3.1 Channel Model in MIMO: Unlike traditional Single-Input-Single-Output (SISO) (Figure 3(a)), a MIMO system (Figure 3(b)) allows for multiple independent transmission channels, without any additional transmitted power or bandwidth. This results in a CC that increases almost linearly with the increase in the number of antenna elements (under specific conditions) [13] [14].

The input-output relationship between the transmitter (T_x) and receiver (R_x) in a MIMO wireless propagation channel with m transmit and n receive antennas is expressed by [1],

$$Y = HX + W \tag{1}$$

where X=[m×1] transmit vector, Y= [n×1] received vector, W= additive white Gaussian noise vector, and H=[n×m] channel matrix composed of the complex random variable, h_{ij} for i=1,…., n and j=1,….m, signifying the channel fading coefficient between the ith receive antenna and jth transmit antenna.

3.2. Path Loss between Transmitter and Receiver: The scattering parameters (S-parameters) between T_x and R_x antennas can be obtained from a vector network analyzer (VNA), which gives the path loss (PL) using equation (1) [15].

$$\mathrm{PL} = \frac{|S_{21}|^2}{(1-|S_{11}|^2)(1-|S_{22}|^2)g_{Tx}g_{Rx}e_p} \tag{2}$$

where S_{21} is the transmission coefficient, S_{11} and S_{22} are the reflection coefficients of T_x and R_x antennas, g_{TX} is the T_x antenna gain, g_{RX} is the R_x antenna gain, and e_p is polarization efficiency (=1 for co-polarized antennas and 0.5 for cross-polarized antennas). In another way, the PL is taken as the path gain factor= $\left(\lambda/_{4\pi D}\right)^2$, here D is the distance between T_x and R_x antennas, and λ is the wavelength. The channel matrix (H) formed between the T_x and R_x antennas is calculated using the PLM as follows [16]:

$$\mathrm{PL} = -10\left(\frac{1}{MN}\sum_f 1 \sum_{i=1}^{M} 1 \sum_{j=1}^{N} \left|H_{i,j}(f)\right|^2\right) \tag{3}$$

where $H_{i,j}(f)$ is the transfer function in frequency-domain for the channel between the jth T_x antenna to ith R_x antenna, so it represents the channel formed between the T_x and R_x antennas, M, N=1, 2, 4,8.

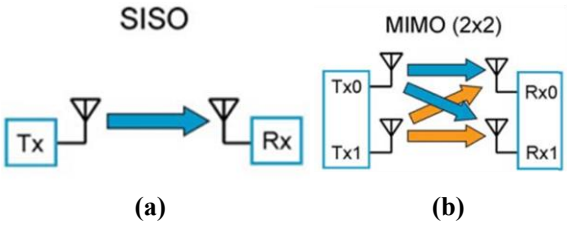

Figure 3: Techniques of channel communications with their CC (a) SISO (b) MIMO.

3.3 Kronecker Model (KM) for H-Matrix: Another model that can be used to construct the H-matrix is the Kronecker model (KM), which assumes that the CC is calculated in the propagation environment of an independent and identically distributed (i.i.d.) Rayleigh fading channel (H_w). This model considered that the complex Gaussian values with zero mean and unit variance make up the entries of the H_w matrix. Using the KM, the MIMO channel matrix H is provided by [17]:

$$\mathrm{H} = R_r^{1/2} H_w R_t^{1/2} \tag{4}$$

where the transmission and reception matrices are denoted by Rt ($=\Lambda^{1/2}\overline{Rr}\ \Lambda^{1/2}$) and Rr ($=\Lambda^{1/2}\overline{Rt}\ \Lambda^{1/2}$), respectively. The complex correlation coefficient is determined by

utilizing the radiation pattern and is indicated by the off-diagonal (i, j) element of the matrix consisting of $\overline{Rr}$ and $\overline{Rt}$, whose diagonal elements are 1. The total efficiency of the ith port (η_{tot}) is represented by the ith element (i, i) of the diagonal matrix Λ [17].

3.4 MIMO CC: From the knowledge of SNR with the transmitting signal, the CC is calculated in 1 Hz of bandwidth using equation (5) from the H-matrix using equation (3) and equation (4) for both models. The CC is expressed as [17]:

$$CC = \log_2[\det(I_{nR} + \frac{SNR}{n_T} HH^*)] \quad (5)$$

where det=determinant, SNR=average SNR, I_{nR}=n_R×n_R identity matrix, H = channel matrix, H*=Hermitian transpose, n_R =number of R_x antennas, and n_T =number of T_x antennas.

4. MIMO Capacity Results:

Further, the channel capacities are evaluated for channels created by $1T_x$×$1R_x$ using Ant. 1, $2T_x$×$2R_x$ using Ant. 2, $4T_x$×$4R_x$ using Ant. 3 with the matched loads connected to the remaining four ports, and $8T_x$×$8R_x$ using Ant. 3 based on both PLM and KM at 5 cm and 25 cm distances between T_x and R_x as shown in Table 3.

Table 3: Channel Details Used for CC Measurement

Name of channel	Type of Antenna used	No. of T_x antennas	No. of R_x antennas	Frequency used (GHz)	Distance (D) between T_x and R_x (cm)
Case 1	**Ant. 1**	**1**	**1**	**2.1-2.8**	**5 and 25**
Case 2	**Ant. 2**	**2**	**2**	**3.1-4.0**	**5 and 25**
Case 3	**Ant. 3**	**4**	**4**	**3.1-4.0**	**5 and 25**
Case 4	**Ant. 3**	**8**	**8**	**3.1-4.0**	**5 and 25**

The measured SNR of the channel formed in Case 1 is presented in Figure 4(a), which shows that the SNR values vary from 16.91dB to 18.38 dB. The measured SNR of the Case 2 and Case 3 are shown in Figure 4(b). The SNR values of Case 2 fluctuate from 26.78 to 29.36 dB and Case 3 varies from 27.27dB to 29.74 dB. The same SNR values are found for Case 4 as in Case 3.

As depicted in Figure 2(a), a pair of Ant. 1 is used to measure the path loss between them at 2.4 GHz. Figure 5 shows the (CC) obtained using PLM based on equations (2), (3) and (4) at two different distances of 5 cm and 25 cm. For both cases, the CC is less than 6 bps/Hz, which is low for the 4G networks whereas, the CC is approximately 3 bps/Hz at two different distances of 5 cm and 25 cm using KM (equations (4) and (5)) as considered only SNR.

The path loss between a pair of dual-polarized circular slot antennas is measured at 3.5 GHz as presented in Figure 2(b). Figure 6 shows the CC obtained from the PLM at 5 cm and 25 cm distances. When D= 5 cm, the CC is obtained from 32 to 34 bps/Hz. However, when D=25 cm, CC is achieved from 34 to 50 bps/Hz. The above data shows that for the frequency range of 3.5 GHz to 3.7 GHz, the CC shows the same kind of pattern for both distances. The CC obtained from the KM is increased from 5 to 13 bps/Hz at a 5 cm distance, while in the case of 25 cm, it fluctuates from 5 to 12 bps/Hz. The above data shows that for the operating band of 3.5 GHz for 5G, the channels can be transmitted with approximately the same CC for both distances.

An 8-port MIMO antenna as shown in Figure 2(c) is used in pairs to obtain the path loss between its various ports. To use as a 4-port antenna-based channel, the path loss between only the top 4-ports of this antenna is used to estimate the H-matrix. Figure 7 compares the CC from the PLM measurements at two different distances of 5 cm and 25 cm. In the case of 5 cm, the CC is obtained from 69 to 79 bps/Hz while in the case of 25 cm, CC fluctuates from 57 to 80 bps/Hz. For the frequency range of 3.5 GHz to 3.7 GHz, the CC shows a similar trend at both distances. When the number of antennas increases from 2 to 4,

there is a slight improvement in CC. In the case of 5 cm, the CC using KM is achieved from 13 to 20 bps/Hz. However, when D=25 cm, CC fluctuates from 5 to 20 bps/Hz.

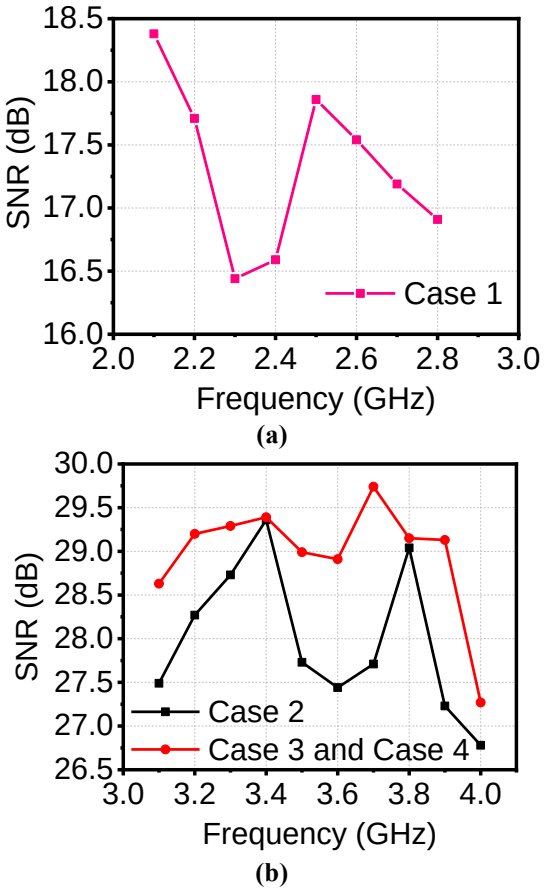

Figure 4: Measured SNR (a) Case 1, and (b) Case 2; Case 3 and Case 4.

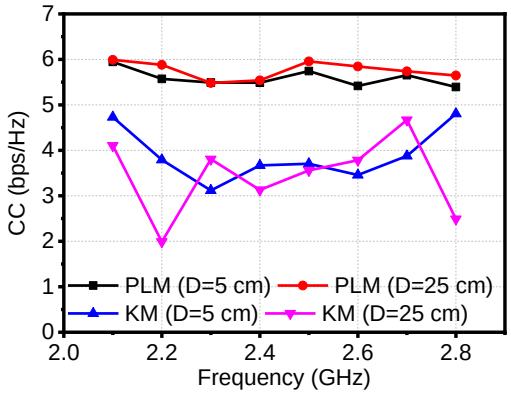

Figure 5: CC for Case 1 using PLM and KM.

Figure 8 shows the CC for channels formed using 8-ports of two identical MIMO antennas at two different distances of 5 cm and 25 cm obtained using PLM. The capacity growth varies from 137 bps/Hz to 157 bps/Hz for a 5 cm distance and from 94 bps/Hz to 135 bps/Hz for a 25 cm distance. In the 3.5 GHz to 3.7 GHz frequency band, the CC exhibits a comparable pattern at both distances. As a result, the CC significantly improves with the addition of eight antennas. Using the KM, the capacity growth varies from as low as 8 bps/Hz to a high value up to 36 bps/Hz in the case of 25 cm, and from 24 bps/Hz to 39 bps/Hz in the case of 5 cm. So, the CC shows a similar trend for both distances in most frequency points.

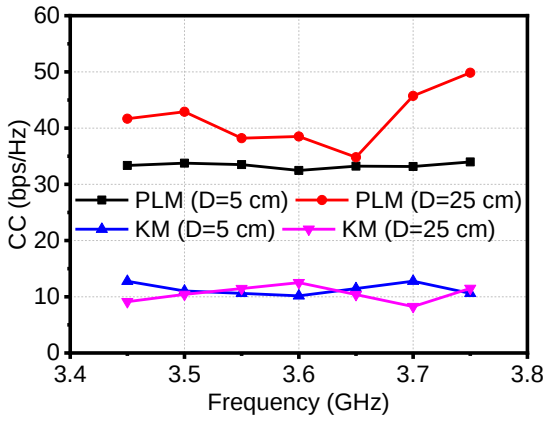

Figure 6: CC for Case 2 using PLM and KM.

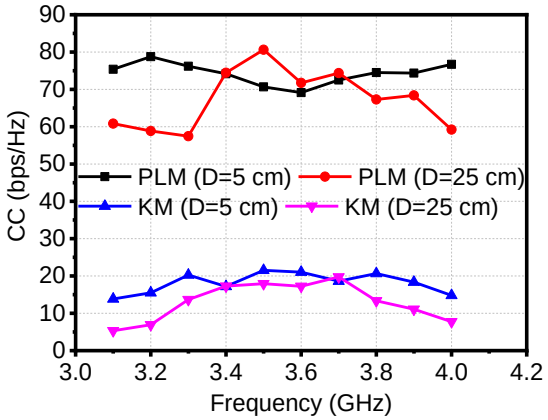

Figure 7: CC for Case 3 (4T×4R) using PLM and KM.

Figure 9 depicts the achievable channel capacities of all four cases at 3.5 GHz using PLM and KM for D=5 cm and 25 cm. It can be noted that the CC calculated using PLM is more than the KM. In Single Input Single Output (SISO) (Case 1), both PLM and KM provide almost the same CC. However, for MIMO Cases 2, 3, and 4, there is a significant difference in the CC. This is because in PLM, real transmission channels were considered which include SNR at both the transmitter's and receiver's end, and in KM, SNR only at the receiver is being considered and it takes care of

the total efficiency while the channel scenario is avoided.

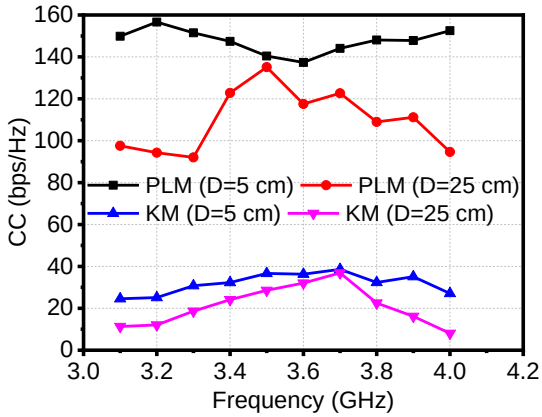

Figure 8: CC for Case 4 (8T×8R) using PLM and KM.

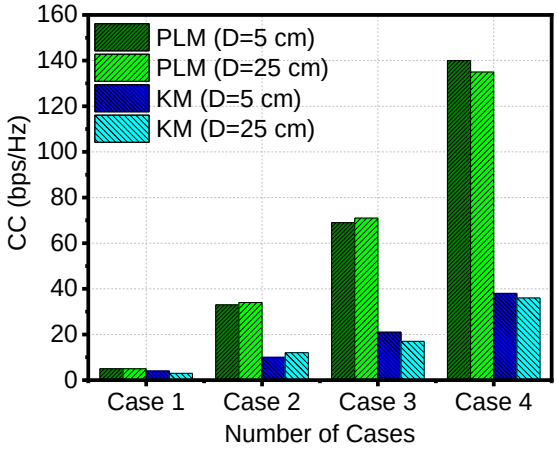

Figure 9: Comparison of channel capacities obtained for the four cases.

Table 4: Comparison of proposed work with other similar previously reported work

Ref.	No. of Antenna Elements	BW (GHz)	Isolation (dB)	Average SNR (dB)	Max. CC (bps/Hz)
[4]	4	2.4-2.44	>12	20 (Set value)	21
[5]	4	27.75-28.18/41.31-41.99	>20	20 (Set value)	21
[6]	4	2.42-7.45	>12	20 (Set value)	21.34
[7]	4	0.356–0.536	>20	20 (Set value)	19.9
[8]	12	3.4-3.6 (-6dB BW)	>10	20 (Set value)	59.87
[9]	2	2.45	NR	30 (Set value)	16
[18]	4	2.9-10.86	>22	NR	NR
[19]	4	3.1-10.6	>17	NR	NR
[20]	4	3.5-11	>17	NR	NR
[21]	4	2.3-13.75	>22	NR	NR
Case 1*	1	2.29-2.95	NA	17.35 (Measured)	PLM=5, KM=4
Case 2*	2	3.4-3.8	>16	28 (Measured)	PLM=34, KM=12
Case 3*	4	3.4-3.8	>15	29 (Measured)	PLM=71, KM=21
Case 4*	8	3.4-3.8	>15	29 (Measured)	PLM=140, KM=38

Note: * = This Work, BW=Bandwidth, and NR=Not Reported.

With the increase in the distance, no significant change in CC is observed for both PLM and KM. This shows that the CC is independent of the distance between T_x and R_x. As the number of T_x and R_x antennas increases, CC increases almost linearly in both PLM and KM. This confirms that the CC is dependent on the number of antennas on both the T_x and R_x sides. These results are important for using MIMO antennas in information and communication technology systems for the Smart City. So, the MIMO antenna with more number of antenna elements provides high data rates.

This work is finally compared with the recently reported work in Table 4, which has calculated CC. In the previous work [4]-[9], SNR is set to a fixed value of 20 dB or 30 dB, while other 4-port MIMO antennas are reported without CC [18]-[21]. None of the previously reported work has measured SNR and calculated CC using PLM and KM. Also, in the proposed work CC is calculated by varying the number of antennas at both T_x and R_x and keeping 5 cm and 25 cm distance between T_x and R_x antennas. Addressing the environmental challenges in outdoor networks faced by antennas used is critical for ensuring their long-term durability and reliability. Environmental factors such as temperature variation, humidity, precipitation, wind, dust, pollution, solar radiation, and atmospheric absorption can significantly impact channel performance in addition to multipath interference.

5. Conclusions: This paper investigates the Channel Capacity (CC) for WLAN and 5G bands at 2.4 GHz and 3.5 GHz bands, respectively, for different channels constructed utilising the 1-port, 2-port, 4-port, and 8-port antennas. Two models are used to evaluate the CC: path loss model (PLM) and Kronecker's model (KM). Because SNR just at the receiver is taken into account in KM, significant discrepancies in results are achieved when compared to those obtained by PLM. In path loss computation, however, genuine transmission channels were taken into account, which include SNR at both the transmitter and receiver's end. Taking into account the impact on the CC in the many source scenarios makes the study valuable for wireless communication systems that use MIMO antennas.

Acknowledgments:
Authors would like to express their gratitude to the Faculty Research Programme (FRP) of the Institute of Eminence (IoE), University of Delhi (Letter Ref. /No./IoE/2023-24/12/FRP dated 31.08.2023)

Conflict of Interest:
Authors declare No conflicts of interest.

References:

[1] M. Qaraqe, Q. H. Abbasi, A. Alomainy and E. Serpedin, "Experimental Evaluation of MIMO Capacity for Ultrawideband Body-Centric Wireless Propagation Channels," *IEEE Antennas and Wireless Propagation Letters,* vol. 13, pp. 495-498, 2014.

[2] A. Ramachandran, S. Mathew, V. Rajan and V. Kesavath, "A Compact Tri band Quad-Element MIMO Antenna Using SRR Ring for High Isolation," *IEEE Antennas and Wireless Propagation Letters,* vol. 16, pp. 1409-1412, 2017.

[3] S. Ramasamy, and A. Madhu, "A Compact Tri-Band MIMO Antenna for WLAN and 5G Applications," *Applied Physics A,* vol. 130, p. 113, 2024.

[4] Y. S. Kim and D. -H. Cho, "Design of Four-Port Integrated Monopole Antenna Using Refraction Effect of Dielectric Medium for Pattern Gain Enhancement," *IEEE Antennas and Wireless Propagation Letters,* vol. 19, no. 4, pp. 621-625, April 2020.

[5] R. N. Tiwari, D. Sharma, P. Singh and P. Kumar, "Design of Dual-Band 4-Port Flexible MIMO Antenna for mm-Wave Technologies and Wearable Electronics," *IEEE Access,* vol. 12, pp. 96649-96659, 2024.

[6] S. K. Mahto, A. K. Singh, R. Sinha, M. Alibakhshikenari, S. Khan and G. Pau,

"High Isolated Four Element MIMO Antenna for ISM/LTE/5G (Sub-6GHz) Applications," *IEEE Access,* vol. 11, pp. 82946-82959, 2023.

[7] A. Iqbal, M. Al-Hasan, I. B. Mabrouk and M. Nedil, "Scalp-Implantable MIMO Antenna for High-Data-Rate Head Implants," *IEEE Antennas and Wireless Propagation Letters,* vol. 20, no. 12, pp. 2529-2533, Dec. 2021.

[8] B. Yang, Y. Xu, J. Tong, Y. Zhang, Y. Feng and Y. Hu, "Tri-Port Antenna With Shared Radiator and Self-Decoupling Characteristic for 5G Smartphone Application," *IEEE Transactions on Antennas and Propagation,* vol. 70, no. 6, pp. 4836-4841, June 2022.

[9] T. Xie et al., "Two-Way Power Divider With Wide Tunable Power Ratio Range for Weighted-Polarization MIMO Antenna in BAN Radios at 2.45 GHz," *IEEE Antennas and Wireless Propagation Letters,* vol. 21, no. 7, pp. 1333-1337, July 2022.

[10] P. Sehgal and K. Patel, "Performance Analysis and Impedance Modeling of Rectangular and Circular Split-Ring Resonator Antennas in 2.4/5.2 GHz Bands," *Progress In Electromagnetic Research C,* vol. 117, pp. 159-171, 2022.

[11] V. Kaushal, A. Birwal, and K. Patel, "Diversity characteristics of four-element ring slot-based MIMO antenna for sub-6-GHz applications," *ETRI Journal,* vol. 45, no. 4, pp. 581-593, 2023.

[12] V. Kaushal, A. Birwal, S. M. Patel, and K. Patel, "Diversified Path Loss Performance of Dual-Polarised MIMO Antenna in Sub-6 GHz for RFID Applications," *International Journal of Electronics,* vol. 111, no. 7, pp. 1196-1212, 2024.

[13] M. A. T. Alrubei, I. A. Alshimaysawe, A. N. Hassan, and A. H. K. Khawayyir, "Capacity Analysis and Performance Comparison of SISO, SIMO, MISO & MIMO Systems," in *Imam Al-Kadhum International Conference for Modern Applications of Information and Communication Technology*, Baghdad, Iraq, 2020.

[14] R. Ullah, S. Ullah, S.Faisal, I. B Mabrouk, M.J Al Hasan and B. Kamal, "A Novel Multi-Band and Multi-Generation (2G, 3G, 4G, and 5G) 9-Elements MIMO Antenna System for 5G Smartphone Applications," *Wireless Networks,* vol. 27, no. 7, pp. 4825-4837, 2021.

[15] V. Kaushal, A. Birwal, S. M. Patel and K. Patel, "Path Loss of Two-Port Circular-Ring Slot Antenna For RFID Applications," in *IEEE International Conference on RFID Technology and Applications (RFID-TA)*, Delhi, 2021.

[16] B. Holter, "On the Capacity of the MIMO Channel: A Tutorial Introduction," in *Int. Proc. IEEE Norwegian Symposium on Signal Processing*, Trondheim, 2001.

[17] B. Clerckx, and C. Oestges, "Analytical MIMO Channel Representations for System Design," in *MIMO Wireless Networks*, Academic Press, Dec. 2013, pp. 59-100.

[18] J. Zhang, C. Du, and R. Wang, "Design of a Four-Port Flexible UWB-MIMO Antenna with High Isolation for Wearable and IoT Applications," *Micromachines,* vol. 13, no. 12, p. 2141, 2022.

[19] T. Govindan, S. K. Palaniswamy, M. Kanagasabai, and S. Kumar, "Design and Analysis of UWB MIMO Antenna for Smart Fabric Communications," *International Journal of Antennas and Propagation,* vol. 2022, no. 1, p. 5307430, 2022.

[20] A. A. Ibrahim, M. I. Ahmed, and M. F. Ahmed, "A systematic investigation of four ports MIMO antenna depending on flexible material for UWB networks," *Scientific reports,* vol. 2022, p. 14351, 2022.

[21] Z. Tang, X. Wu, J. Zhan, S. Hu, Z. Xi and Y. Liu, "Compact UWB-MIMO Antenna With High Isolation and Triple Band-Notched Characteristics," *IEEE Access,* vol. 7, pp. 19856-19865, 2019.